

Screen-printed electrochemical sensors and biosensors for detection of biomarkers

Ava Gevaerd^{a,b}, Tiago Almeida Silva^c, Luiz R. G. Silva^d, Luiz H. Marcolino-Junior^a,
Márcio F. Bergamini^a, Bruno Campos Janegitz^{d*}

*^aLaboratório de Sensores Eletroquímicos (LabSensE), Departamento de Química,
Universidade Federal do Paraná (UFPR), Curitiba, Paraná, 81531-980, Brazil.*

^bHilab, Rua José Altair Possebom, 800, Curitiba, Paraná, 81270-185, Brazil.

*^cDepartment of Chemistry, Federal University of Viçosa, Viçosa, Minas Gerais, 36570-
900, Brazil.*

*^dLaboratory of Sensors, Nanomedicine, and Nanostructured Materials, Federal
University of São Carlos, Araras, São Paulo, 13600-970, Brazil.*

*Corresponding author:
Prof. Bruno C. Janegitz
E-mail: brunocj@ufscar.br

Summary

Abstract.....	3
1. Introduction	4
1.1. Biomarkers.....	4
1.2. 2D-printed electrochemical devices.....	6
2. Electrochemical determination of biomarkers using 2D printed devices.....	13
3. Conclusions and Future Perspectives	25
Acknowledgment.....	25
References	25

Abstract

In this chapter, the use of miniaturized 2D printed electrochemical devices for the detection of biomarkers is explored. This section reports the different types and forms of construction of 2D electrochemical devices, as well as their architecture, employed materials and production methods. In addition, different models are explored, such as electrodes obtained by screening, made from stamps and wearable sensors, including the modification with anchoring of different species, such as thin films, metallic nanoparticles, DNA strands, antibodies, enzymes, among others. Furthermore, the application of the devices and their advantages will be discussed in detail, as well as the future prospects for the use of these devices.

Keywords: 2D-printing; electrochemistry; biomarkers; screen-printed electrodes; biosensors.

1. Introduction

The monitoring of biomarkers in clinical practice as well in laboratory researches has been widely employed over the last years due to its presence and/or concentration level be accepted almost without question as a primary endpoint in several clinical trials. With the integration of different systems, it is possible to create a variety of devices that bring together several functions for an analytical procedure. Also, with the advancement of micro and nano technologies is possible to build platforms that come closer and closer to the dimensions of the biological world, facilitating the study and determination of some biological systems, processes, and species. This fact explains the great worldwide interest in the study of the so-called Miniaturized Electroanalytical Devices systems produced based on 2D platforms, which encourage this chapter.

1.1. Biomarkers

Biomarkers refer to measurable biological parameters and quantifiable that can serve as indicators for related assessments to health and patient physiology. A target biomolecule can be detected in the blood or other body fluid that is associated with a sign of a normal or abnormal process, or of a condition or disease can be used as a biomarker. The use of biomarkers for clinical analysis purposes is easier and cheaper than directly measuring the “final disease”, with the advantage of the possibility of measurement and determination in a shorter period since these marker species usually reveal themselves in advance.

They can be used in the tracking, diagnosis, characterization, and monitoring of diseases; as prognostic indicators and for therapeutic interventions; to predict and treat adverse drug reactions, as well provide further information on the disease or intervention into account, among other possibilities (Figure 1). Good biomarkers should be measured with little or no variability, should be a signal ratio, and can meet several criteria for different uses or exhibits specific characteristics that allow its particular use [1].

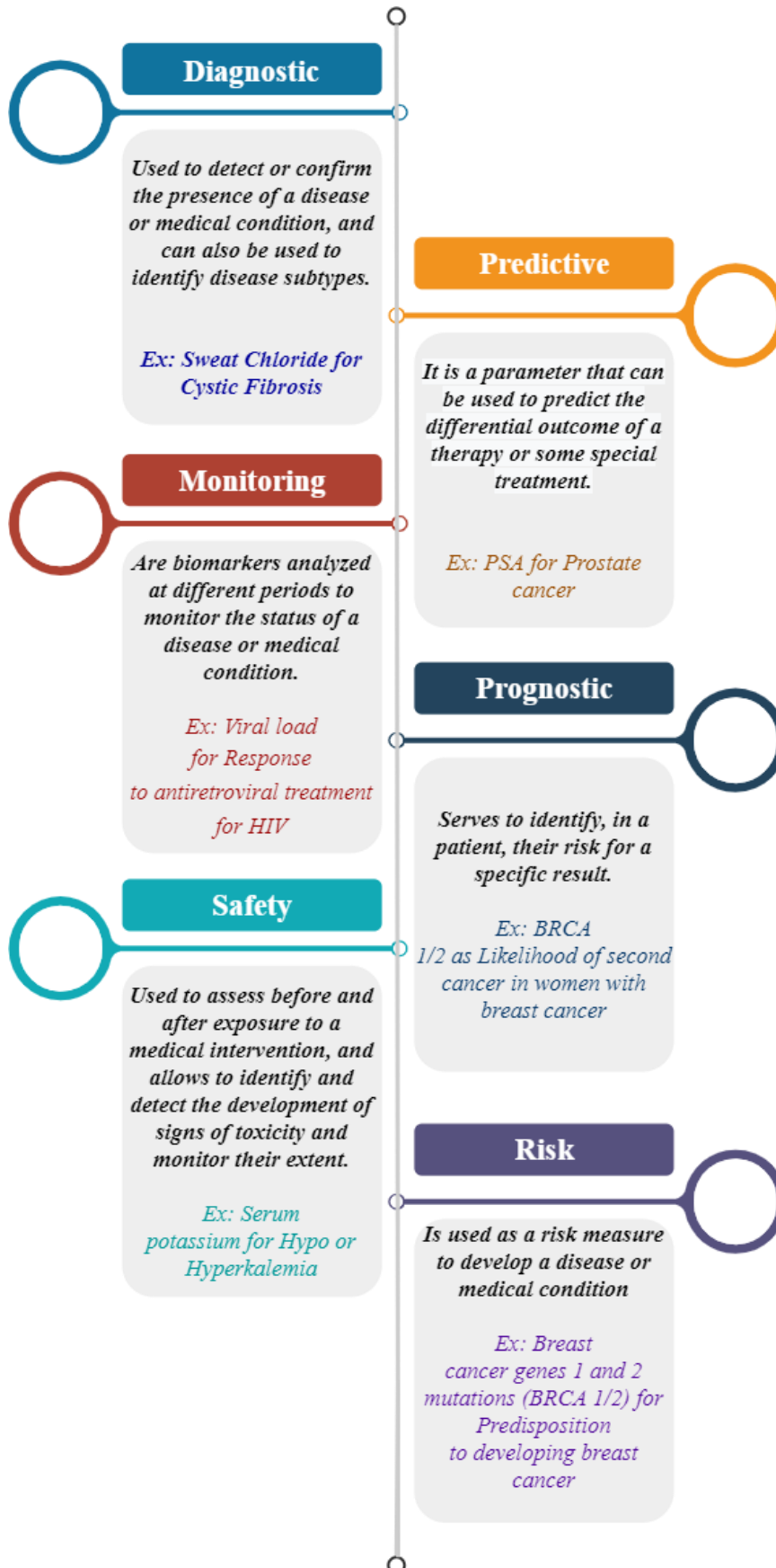


Figure 1. Types of Biomarkers. Adapted from [1].

Pletcher et al. [2] describe that there are three fundamental mechanisms, in the context of clinical care, based on the determination, measurement, and quantification of a biomarker that can improve an individual's health. Figure shows a representative scheme of the mechanisms described by the authors, which are: help the patient to understand their illness or disease risk and thus directly improve their quality of life and/or mental health; motivate the patient to make behavioral changes that improve health; help a doctor to make a better clinical decision about the use of a treatment that leads to an improvement in the patient's health. The goal of determining biomarkers is to develop screening tests that can detect diseases before the evolution of symptoms or at a stage where they are most effectively treated since altered levels in specific types of biomarkers can be closely related to several illnesses [3,4].

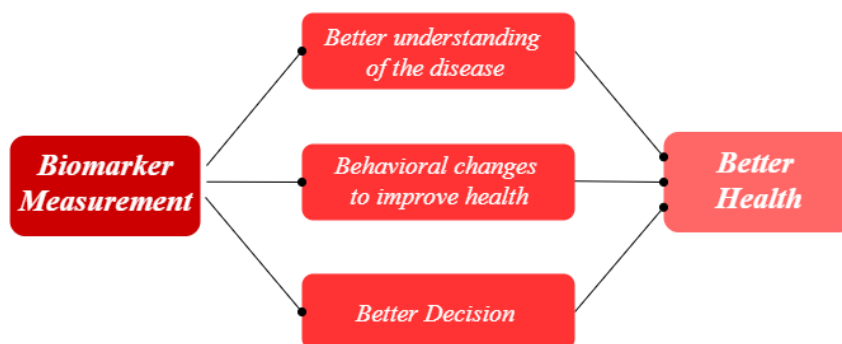


Figure 2. Goals for biomarker determination based on Pletcher et al. [2]

Biological fluids (e.g. blood, saliva, and urine) are the most used samples in laboratory tests and provide useful biological information for the monitoring of various diseases. They are composed of a wide range of biomolecules, such as enzymes, hormones, carbohydrates, nucleic acids, proteins, lipids, salts, and various other organic and inorganic compounds that can be used as biomarkers that reflect and indicate an individual health status.

Each class is vital in the day-to-day activities of each organism and therefore continuous monitoring of levels is essential. The imbalance, whether due to the absence or excess of these species in the living organism, causes a series of biological disorders to appear, such as Alzheimer's disease, Parkinson's disease, diabetes, heart attack, pregnancy complications, osteoporosis, etc. There are hundreds of cataloged biomarkers described in the literature, and to be useful in diagnosis, biomarkers need to provide sufficiently high levels of sensitivity and specificity in detecting and correctly classifying distinct disorders. [5] In addition, biomarkers must be reproducible, reliable, inexpensive, non-invasive, and easily accessible to ensure their application in daily clinical practice.

1.2. 2D-printed electrochemical devices

The search for different platforms for the detection of biomarkers has been a great motivation for research in analytical chemistry. There is a growing demand for devices able to offer continuous and fast response and stable measurements using small volumes and low concentration samples. Such studies also point to the development of systems with characteristics of portability and ease of use and are closely linked to another trend with considerable relevance within the scope of analytical chemistry, which is miniaturization. [6,7]

The concept involves the sensors and biosensors miniaturization since they can be also coupled to miniaturized sample pre-processing and detection systems.

Electrochemical techniques end up appearing as a promising and highly recommended set of transducers for miniaturized sensors and biosensors. In general, electrochemical transduction can be characterized by its rapid response, high analytical sensitivity, wide linearity, repeatability, and adaptability to miniaturized and portable analysis systems. The availability of commercial electrochemical instrumentation adapted for fieldwork also emphasizes the role of electrochemical techniques in the search for more robust and efficient miniaturized devices.

For the manufacture of electrochemical detection devices that meet the above requirements and that make use of low-cost materials, the technique based on 2D printing has been increasingly explored. Through the application of this technology, it is possible to design complete electrochemical measurement systems, in an easy and scalable way, and that present functional characteristics of operation and design according to the demand to be used. Thus, the most relevant technical aspects about the fabrication and evaluation of electrochemical devices manufactured by 2D printing are discussed below.

The purpose of 2D printing is directed to the manufacture of screen-printed electrodes, among the different possibilities, screen printing (SP) is an appropriate strategy for the preparation of conductive films on an inert support (glass, ceramic, or polymer) [8]. The use of this strategy involves simple and inexpensive equipment and processes, yet providing a highly reproducible manufacturing method, the SP has proven highly compatible for the development of disposable sensors since the 1990s. A classic configuration of SPEs is shown in Fig. 3. In this case, the SPE has typical dimensions of $3 \times 1 \times 0.05$ cm and consists of three electrodes: working electrode (WE), counter electrode (CE), and pseudo-reference electrode (PRE). Despite this typical configuration, available from various manufacturers, laboratory protocols can be implemented to obtain other designs. Within this context, sensors/detectors employed for analytical purposes stand out as one of the lines of research that can most evolve with the use of these technologies [9,10].

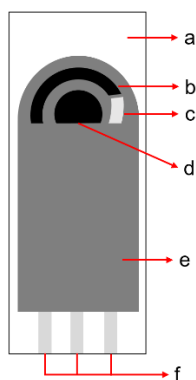


Figure 3. Representation of a typical SPE configuration: (a) inert solid substrate; (b) counter electrode; (c) pseudo reference electrode; (d) working electrode; (e) insulator layer; (f) conducting paths for connection. (Adapted from [11]).

The main 2D printing methods employed to manufacture electrodes and electrochemical devices include inkjet printing, screen-printing, and roll-to-roll (R2R) printing. The basic working principle of each of these techniques can be seen in the schemes of Fig. 4. Inkjet printing is a droplet-ejection-based technique, which droplets are typically generated either by piezoelectric actuation (piezoelectric inkjet printing) or thermally (thermal inkjet printing) [12]. The inkjet printers can be operated in drop-on-demand or continuous modes, as distinguished in Figs. 4 (a). In the drop-on-demand inkjet printing mode, the target substrate is maintained on a fixed position while a

moveable print head ejects droplets at the desired positions [12]. On the other hand, in the continuous mode, the fixed and moving parts are inverted, i.e., a fixed print head provides a constant stream of droplets on the moveable target substrate being, therefore, a preferred operation mode for industrial applications [12]. In the case of screen-printing, it is carried out by using a stencil screen (made of a mesh of silk, fabric, synthetic fibers, or metal threads) [13]. Thus, the moving of a roller or squeegee across the screen ensures the passage of the ink through the threads of the woven mesh and reaching the inert solid support of the print. Fig. 4 (b) illustrates the screen-printing process. To increase productivity, the R2D printing method outlined in Fig. 4 (c) can be adapted. Another approach for obtaining 2D-printed electrodes was reported by Windmiller et al. [14] using the pattern-transfer technique. Fig. 5 details the steps involved in the stamp-transfer fabrication of electrodes. By using this simple and low-cost technique, sensors and biosensors can be directly prepared on different types of irregular surfaces and with different morphologies.

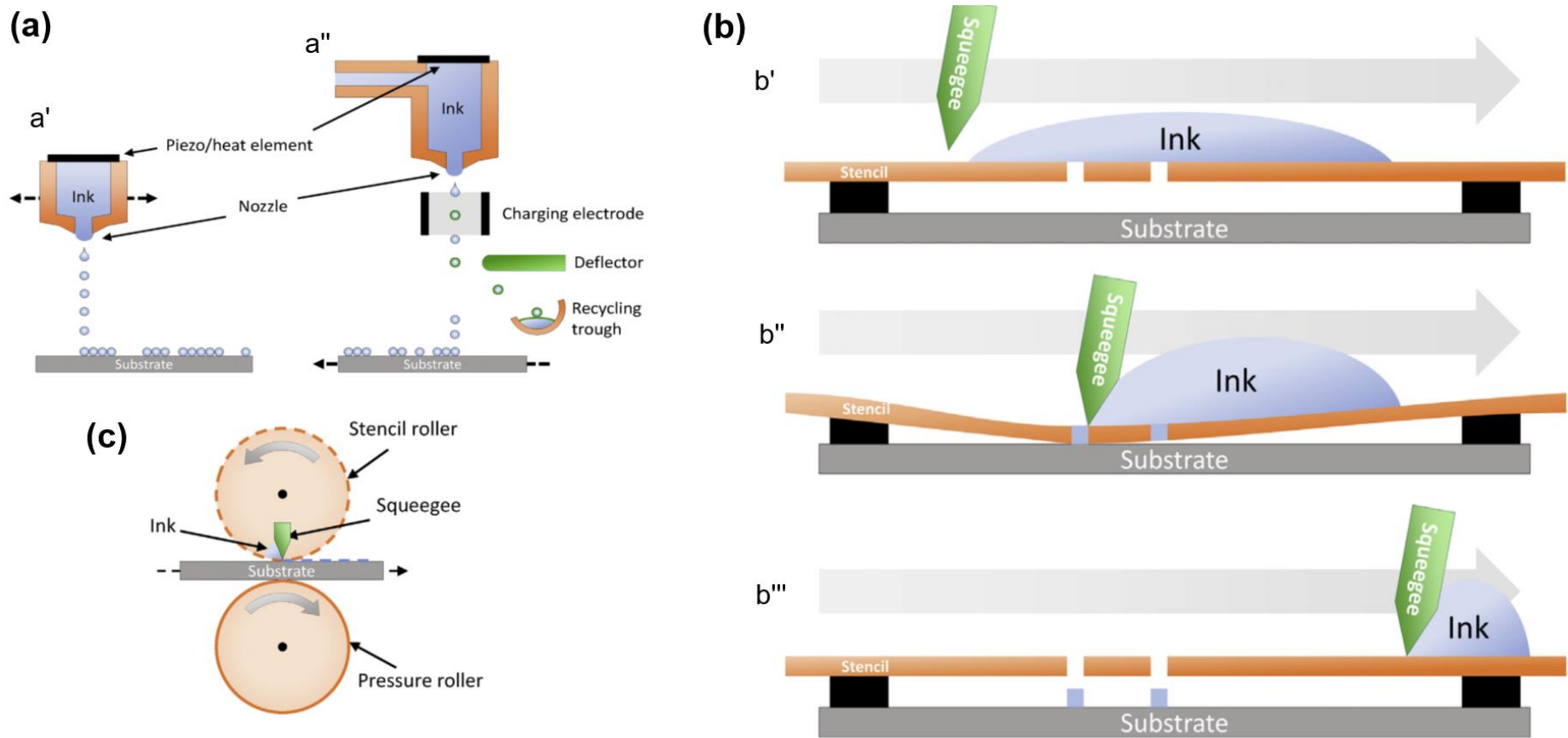


Figure 4. Illustration of (a) inkjet printing (drop-on-demand (a') and continuous (a'')); (b) screen printing process: (b') printing ink on the stencil is moved across the stencil with a squeegee and (b'') deposited through voids in the stencil, (b''') after the stencil is lifted off, the printed pattern remains on the substrate.; (c) roll-to-roll screen printing. (Reprinted from [12] with permission of Elsevier).

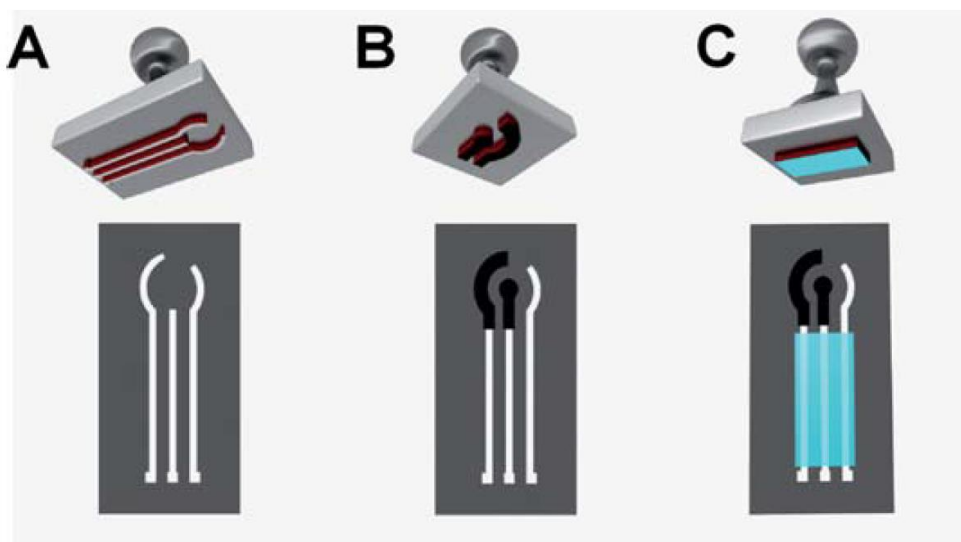


Figure 5. Illustration detailing the steps involved in the stamp-transfer preparation of a common electrode pattern using elastomeric stamps with custom-designed surface reliefs containing the electrode pattern (top): (a) Ag/AgCl conductor layer, (b) carbon active layer, and (c) insulator layer (Reproduced from [14] with permission from the Royal Society of Chemistry).

In preparing the SPEs, a conductive ink with appropriate viscosity (of 3.0 to 10 Pa s) is forced to flow through a screen, which defines the shape and size of the desired electrodes [11]. Different stencil screens are normally prepared to print the different parts of the SPE and, the printing is performed sequentially after the thermal drying and curing of the previous layer. Thus, the manufacturing process of SPEs involves choosing the desired design for the printing screen and the materials (ink and substrate) and studying any subsequent modifications of the surface of the electrodes via chemical and/or electrochemical treatment, or deposition of thin films of nanomaterials or biological recognition species.

Considering the steps involved in the preparation of SPEs, numerous researches have been developed to study new compositions of conductive inks, as well as printing solid substrates, always aiming at high analytical performance associated with the use of cheaper and less toxic alternative materials. As for the substrate, great prominence can be offered to SPEs based on paper and polymers. Both give rise to flexible and disposable electrodes, whose adhesion (especially in the case of paper) of the conductive ink is very efficient. Moreover, paper is biodegradable and polymers from recycling sources (such as polyethylene terephthalate (PET) from soda bottles) can be used, which are both especially important features in the context of environmental preservation.

Focusing on the solid plastic substrates for SPEs, recently, the reuse of PET from drink bottles as the substrate for the screen printing of disposable SPEs has been reported. An alternative low-cost carbon ink based on graphite powder and nail polish [15] has been used for electrode preparation. The flexible SPEs manufactured by this method were successfully applied at the voltammetric sensing of hydroquinone, epinephrine, and serotonin. Another alternative strategy for SPEs preparation on plastic substrates was recently developed by Faria and collaborators [16]. In this case, an all-plastic disposable electrochemical cell (DCell) was designed and manufactured using a home-cut printer. A template was prepared by cutting an adhesive vinyl, which is transfer to the transparency sheet (polyester). Electrodes are printed on substrate using carbon or Ag/AgCl ink. Fig. 6 outlines the steps of the proposed methodology.

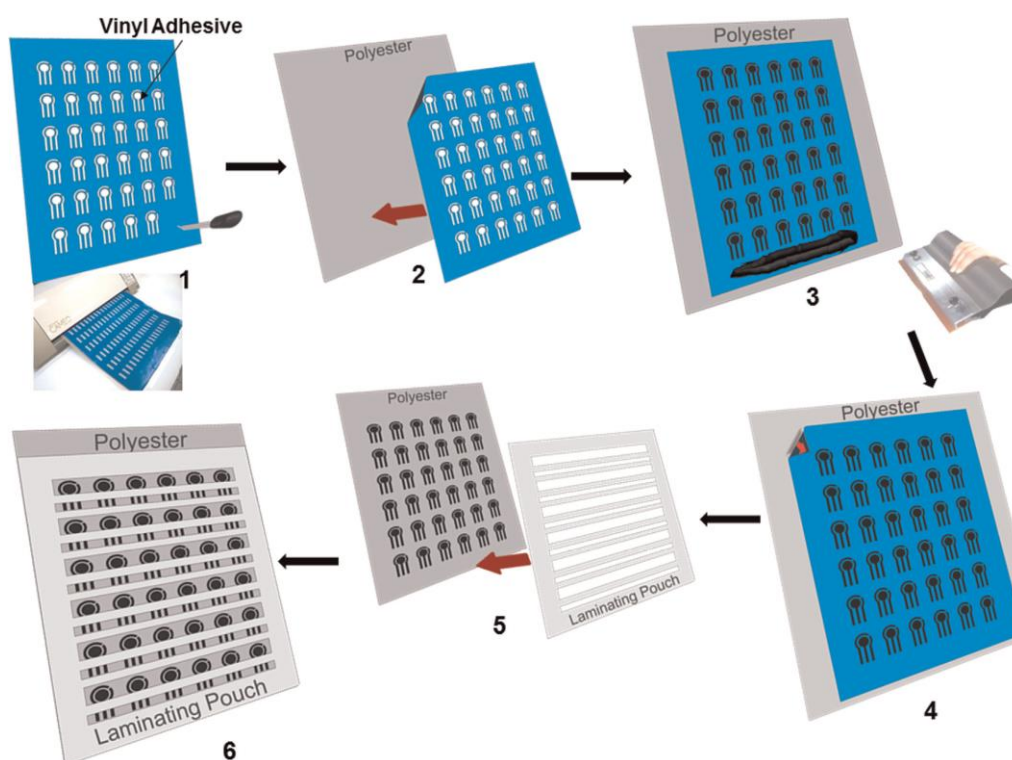


Figure 6. (a) Schematic representation of DCell fabrication: (1) preparation of the template by cutting the adhesive vinyl; (2) transfer of the vinyl to the transparency sheet; (3) carbon ink screen-printing, followed by Ag/AgCl ink deposition; (4) removal of the adhesive vinyl; (5) positioning of the lamination pouch on the printed electrodes, following by heating and pressing; and (6) the DCell ready for use. (Reprinted from [16] with permission of Elsevier).

On the use of paper as a substrate for the direct printing of SPEs, Cinti et al. [17] investigated the manufacturing of SPEs using three different types of paper normally not applied at electrochemistry fields. The evaluated substrates were paper towel, waxed paper, and Parafilm M®. Fig. 7 provides pictures and the dimensions of the manufactured SPEs. The SPEs were manually screen-printed using two masks (masks 1 and 2) and a squeegee. Using mask 1, connections and pseudo-reference electrode were printed; then, mask 2 was used to screen print the working (diameter of 4 mm) and counter electrodes by applying a commercial carbon ink; to finish, the SPEs were cured at mild heating (60 °C for 30 min) to prevent the damage of the paper substrate. In this context, the authors observed an apparent better performance of those SPEs based on towel paper, with an enhanced voltammetric response after the incorporation of cost-effective carbon black (CB) nanoparticles on the working electrode. In the context of SPEs manufactured on paper substrates, it is worth commenting on a recent trend related to the use of pencil/pen drawn electrodes [18]. In this case, the electrodes are manually drawn using commercially available graphite pencils [19], or ballpoint pens are adapted to directly dispense the conductive ink on the paper surface [20]. Toner lines or stencils can be used to delimit the geometry and areas of the electrodes [18]. The simplicity of these printing methods is impressive, however, the fact that they are performed manually can compromise the reproducibility of manufacturing, which would difficult to scale up them for mass SPE production [18].

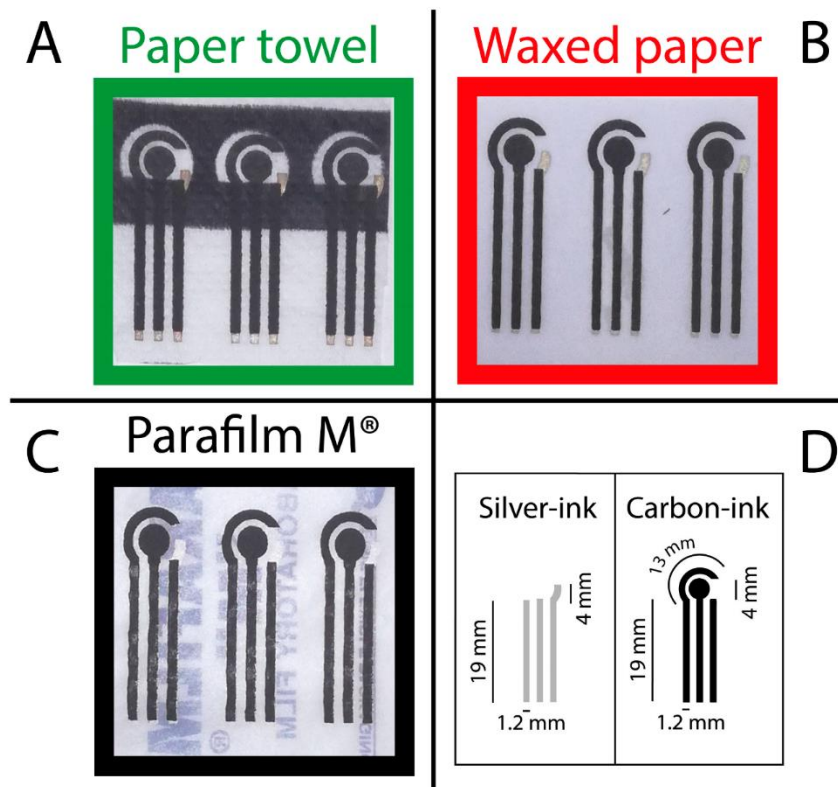


Figure 7. Photographs of electrodes screen-printed on (a) paper towel; (b) waxed paper; and (c) Parafilm®; (d) Dimensions of the conductive tracks that have been screen-printed. (Reprinted from [17] with permission of Royal Society of Chemistry).

In addition to the substrate, conductive ink is a crucial component in making SPEs. The conductive inks applied are those classically used in various electronic components, consisting of three main chemical components: conductive material, binder, and solvent [21]. Each of these components aims to meet specific prerequisites for the desired application, such as high electrical conductivity, ink homogeneity, and the formation of well-adherent coatings on the substrates of interest. Regarding the binder agent, several surfactants and polymers have been used and act as a stabilizer for the ink [21]. Organic solvents (e.g., toluene, isophorone, acetone, etc.) provide important advantages as ease of application, low viscosity, and fast drying. However, the toxicity and high costs associated with the organic solvents make it difficult to use them on a large scale, and efforts have been expended on the formulation of eco-friendly aqueous inks [22]. In the case of the conductive material, these can be carbon-based material and/or metallic species. Special emphasis can be placed on graphite-based carbon conductive inks due to adequate electrical and thermal conductivities, wide availability, and the low cost of this material. Graphite-based SPEs, due to the presence of polymers as the ink binders, often insulating, it could be necessary to carry out chemical and/or electrochemical pre-treatments to activate the electrode surface from the removal of the polymer matrix at the interfacial region (electrode/solution) [23]. Other carbonaceous materials are also explored for the formulation of conductive inks besides graphite, such as the conductive inks based on graphene [24], carbon nanotubes [25], and carbon black [26,27]. In addition to carbon-based conductive inks, there are also conductive inks consisting on dispersions of noble metal nanoparticles (mainly AuNPs [28], AgNPs [29], PtNPs [30] and CuNPs [31]). AgNPs-based inks are most widely used, especially in the preparation of pseudo-reference electrodes, however, in fact, one sees a preference for carbonaceous conductive inks due to the lower production cost. An important aspect of the preparation of

conductive inks is their homogeneity. To ensure this aspect and the reproducibility of electrode construction, protocols involving ultrasonication [32] or double asymmetric centrifugation [33] have been implemented. Practical details and perspectives on preparing conductive inks for printed electrochemical devices can be found in our very recently published review article [21].

SPEs can be applied directly or undergo a preliminary modification step. This modification can take place in the manufacturing process by incorporating the modifier in the conductive ink formulation or as a further modification step by drop-casting, dip-coating, or spin-coating of a solvent-modifier mixture, or even via electrodeposition, electrospray, and electrospun [34,35]. Nanostructured materials are well explored to improve the analytical response of sensors and biosensors based on SPEs, highlighting the use of carbonaceous nanomaterials (carbon black, carbon nanotubes, graphene among others), ionic liquids, metallic and metallic oxide nanoparticles, magnetic nanoparticles, and conductive polymers [34]. The modification of the surface of SPE has been gained attention since it is the feasible platform for the preparation of electrochemical sensors with low-cost and high analytical performance. Among several modifiers, the use of biological species such as enzymes, nucleic acids, and antibodies/antigens allowed the development of enzymatic biosensors, genosensors, and immunosensors for the determination of important biomarkers. The biological recognition site can be immobilized onto the surface of the WE through different physical (e.g., adsorption and entrapment) and chemical (e.g., crosslinking and covalent attachment) methods [11].

2. Electrochemical determination of biomarkers using 2D printed devices

Throughout this section, the recent scientific advances in the use of electrochemical devices obtained by 2D printing will be discussed. The number of contributions in the literature is quite significant, therefore, it is not the intention to exhaust the literature, but to point out promising results from the last years, bringing new perspectives to this important field of research. In Table 1, the reviewed papers dedicated to the development and application of 2D electrochemical devices for the determination of biomarkers are organized. Featuring by the presence on the sensing surface of a biorecognition agent, the electrochemical biosensors currently tend to be preferred when it comes to detecting biomarkers due to their superior selectivity and specificity. An overview of this table shows the applicability of 2D printed electrodes for the incorporation of different types of recognition agents (enzymes, DNA, and antibodies/antigens) in addition to various nanostructured architectures, for the voltammetric, (chrono)amperometric, impedimetric, and/or coulometric detection of biomarkers related to various diseases (e.g. cancers, Alzheimer's and diabetes). The main sample matrix subject to electrochemical analysis is human serum samples from healthy and sick patients. The recent researches use commercial printed or laboratory-manufactured electrodes with classic formats to more complex electrode arrays in microfluidic systems, allowing the multiplexed determination of biomarkers and, including the proposition of flexible and wearable devices coupled to portable potentiostats equipped with a system of real-time data transmission. These general first observations can be better visualized in the following lines, where some advances mentioned briefly are better detailed to the reader.

In the scenario of diabetes control, a novel electroanalytical approach to evaluate diabetic kidney disease (DKD) has been proposed by Smith et al. [36]. In this case, a three-working electrodes configuration of SPCE was adopted to design a disposable electrochemical biosensor for the detection of microRNA (specifically miR-21) DKD

biomarker at patient urine samples. For the biosensor construction, the carbon-based working electrode surface was primarily modified from the electrochemical deposition of 4-amino-3-hydroxy-1-naphthalene sulfonic acid (ANSA), which was then chemically converted into a sulfonyl chloride (ANSCl). After, a 5'-amine-tagged miRNA-specific DNA oligonucleotide was attached via a sulfonamide linkage to complete the biosensor construction. The miR-21 concentration was monitored through chronocoulometric measurements carried out with negative and positive potential sweeps in the presence of the ferri/ferrocyanide redox couple.

Illustrating the use of nano-modified SPEs at the design immunosensors for biomarkers detections, Chanarsa et al. [37] have recently proposed the use of a silver nanoparticles (AgNPs)-reduced graphene oxide (rGO) nanocomposite synthesized by the one-pot wet chemical process for both the SPE modification and analytical signal generation (label-free approach). The scheme of preparation of the biosensor is displayed in Fig. 8. Thus, briefly, the working electrode surface of the SPCE is first modified by drop-casting using an AgNPs-rGO dispersion, followed by incubation periods, and washing steps with PBS buffer to remove unbonded molecules, to sequentially incorporate onto AgNPs-rGO modified-electrode anti-IgG antibodies, BSA (block non-specific binding sites) and target IgG model biomarker. The typical anodic peak for AgNPs, corresponding to the $\text{Ag}^0 \rightarrow \text{Ag}^+ + \text{e}^-$, was explored to the label-free monitoring of IgG model biomarker. As the demonstrative square-wave voltammograms (SWV) of Fig. 8 suggests, the anodic peak current of the AgNPs process suffered deflection in the presence of the analyte, and this signal drop is proportional to the biomarker concentration. Using this strategy, the label-free biosensor provided a low limit of detection (LOD), ensuring the detection of IgG in human serum samples.

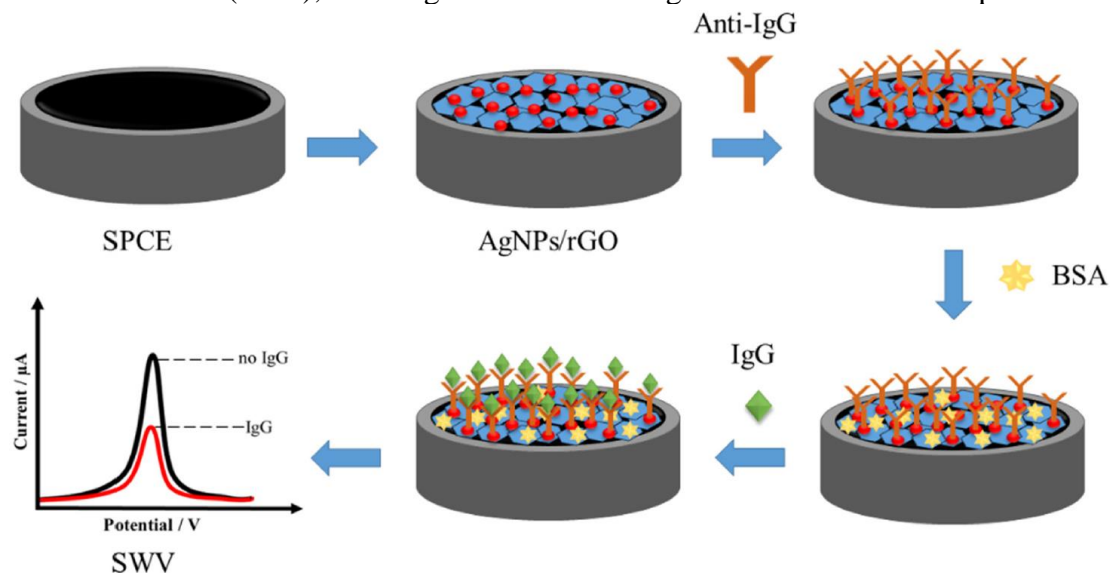


Figure 8. Fabrication of AgNP/rGO-based electrochemical immunosensor. (Reprinted from Ref. [37] with permission of Frontiers).

Besides using three or dual screen-printed electrodes, indeed, the application of 2D printed (bio)sensors consisting of multiple working electrodes coupled to microfluidic paths is an important and current trend. In this scenario, some interesting achievements were reported by Proença et al. [38], who proposed a disposable microfluidic immunoarray device (μID) based on $\text{Co}_{0.25}\text{Zn}_{0.75}\text{Fe}_2\text{O}_4$ nanoparticles (CoZnFeONPs) as peroxidase mimics for the early diagnosis of cancer from the detection of CYFRA 21-1 biomarker. Fig. 9 shows a picture from the disposable microfluidic system composed of

SPCEs with 8 working electrodes, one counter electrode, and one Ag/AgCl pseudo reference electrode. Additionally, in practical terms, the method was able to detect CYFRA 21-1 in real serum samples of healthy and prostate cancer patients, with good correlation with results obtained from an enzyme-linked immunosorbent assay (ELISA).

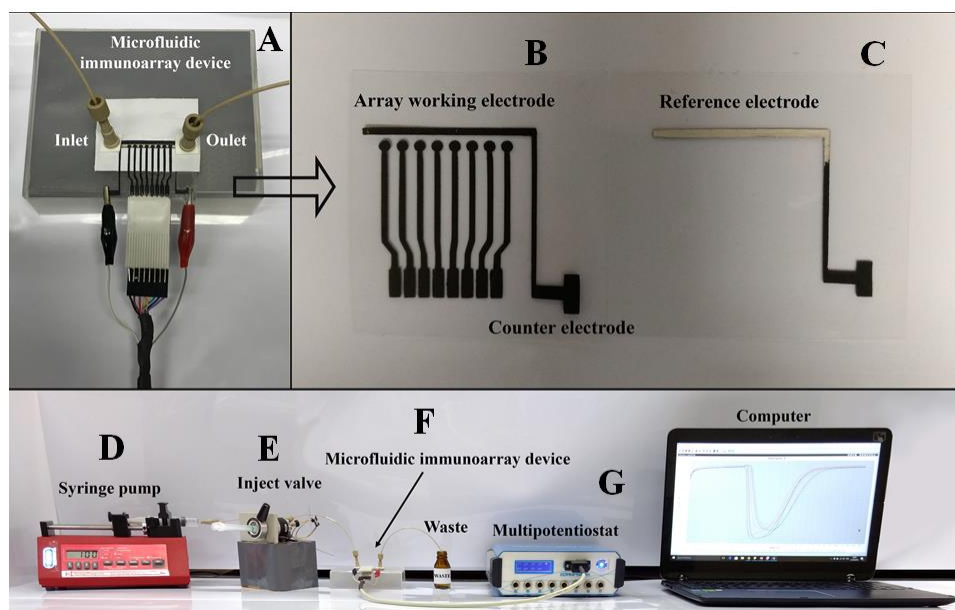


Figure 9. Pictures of the disposable microfluidic device and the setup of the system: (A) disposable microfluidic immunoarray; (B) 8-working electrodes and auxiliary electrode; and (C) reference electrode. The microfluidic system was composed of (D) syringe pump, (E) manual injection valve, (F) disposable microfluidic immunoarray, and (G) multipotentiostat. All parts were connected by using PEEK tubing. (Reprinted from [38] with permission of Elsevier).

In another recent application, the early diagnosis of Alzheimer's disease (AD) was reported by Oliveira et al. [39], where the immunomagnetic capture of the target protein (ADAM10 protein, as a potential AD biomarker) and separation from the biological sample was employed as a part of the established biosensing procedure. Fig. 10 outlines the involved steps, including the functionalization of magnetic beads (MB) with horseradish peroxidase (HRP) as a label and anti-ADAM10 antibodies (Fig. 10 (a)), ADAM10 immunomagnetic capture in the sample, and injection of pre-treated samples in the microfluidic system coupled to an electrochemical detector.

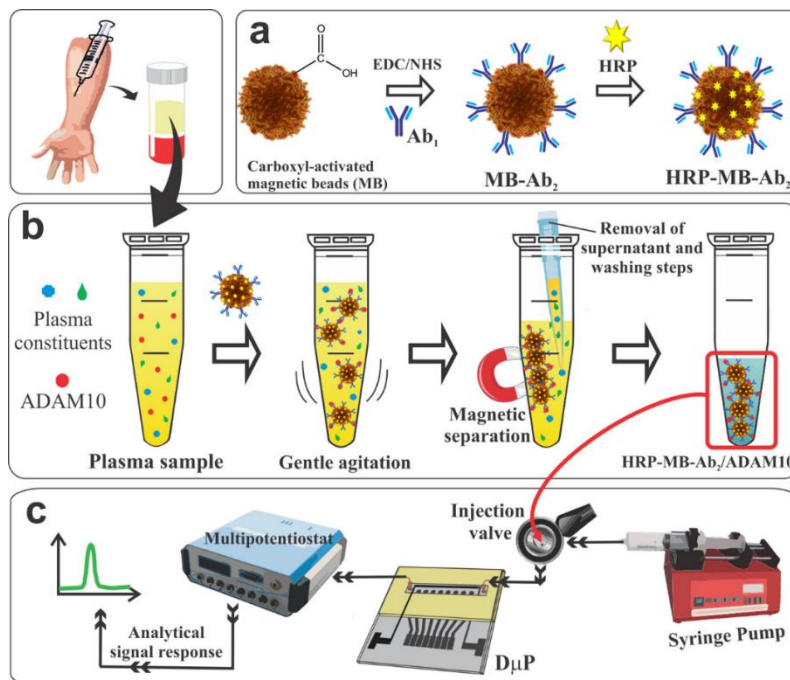


Figure 10. Immunomagnetic capture of ADAM10 in a plasma sample and the detection using $D\mu P$. (a) Conjugation of the MBs with HRP and Ab_2 . (b) ADAM10 immunomagnetic capture in the sample. (c) Setup of the microfluidic system and the transient current signal. (Reprinted with permission from [39], Copyright (2020), American Chemical Society).

Still in the scenario of 2D-printed electrochemical devices with multiple electrodes, suitable for multiplexed analyses, Fava et al. [40] has proposed a disposable microfluidic electrochemical paper-based device based on sixteen independent microfluidic channels with electrochemical detection. The design of the parts of the device containing the working electrodes, counter electrodes and pseudo reference electrodes are presented in Figs. 11 (a) and (b). The assembly of the device and a picture from the final device can be seen in Figs. 11 (c) and (d). Once again, the printing cut process was used to obtain the formats and masks for applying the carbon conductive ink. With this device, a small aliquot of the sample ($60 \mu\text{L}$) is injected into the central hole of the device, which flows through the paper microfluidic channels until reaching the 16 cells (sensing spots) circularly arranged (Fig. 11 (e)). The working electrodes can be functionalized in the most varied ways to obtain multiple sensors and biosensors. For now, the modification of working electrodes with carbon black (CB) nanoparticles and the determination of biomarkers (glucose, creatinine, and uric acid) in real urine samples has been reported [41].

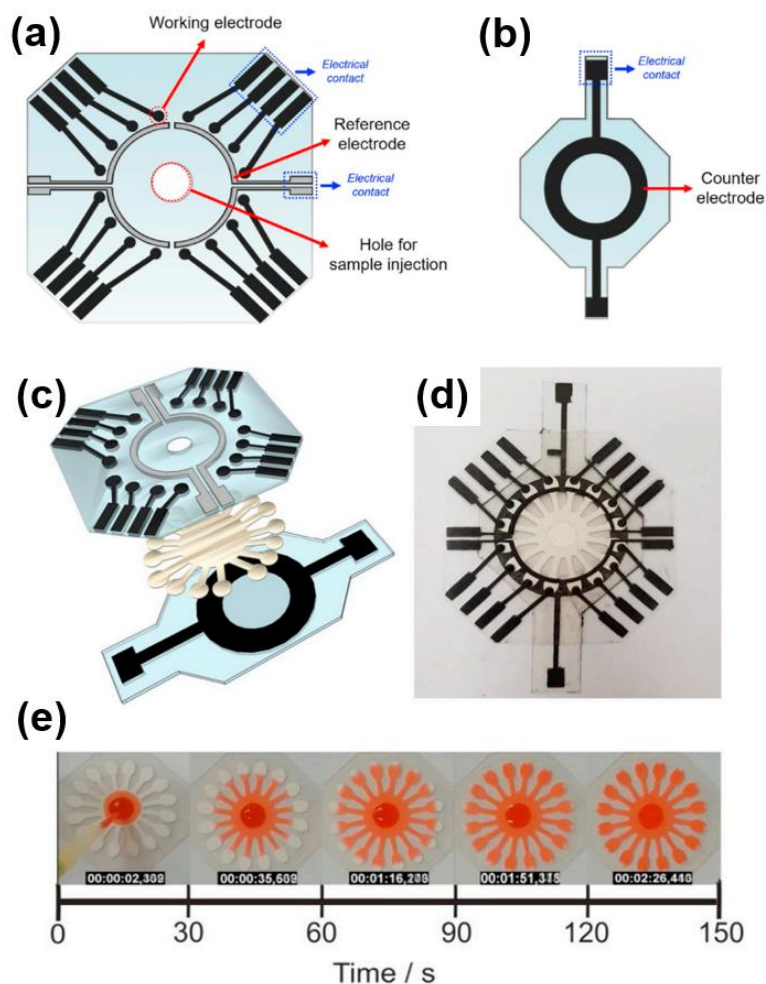


Figure 11. Design of the (a) WEs/REs and (b) CE layers. (c) Steps for device layer assembly. (d) Photography of assembled microfluidic paper-based electrochemical device. (e) Homogeneous elution of $1.0 \times 10^{-3} \text{ mol L}^{-1}$ Allura red dye solution in the microfluidic pathway. (Reprinted from [40] with permission of Elsevier).

To produce analysis methods that are less invasive and generate real-time results, 2D printing technologies have provided important contributions to the field of wearable (bio)sensors. Several approaches can be found in the literature, such as the technology recently reported by Vinoth et al. [42]. The authors developed a wearable microfluidic sensor using a screen-printed carbon master for the multiplexed analysis of biomarkers at sweat during exercise activities (Fig. 12). The sweat sampling and sensing steps are taken in a low-dimensional microdevice containing silane functionalized microchannels, which enhance the sweat collecting at the inlet and the directing of samples to the surface of the printed sensor. For the electrochemical transduction (amperometry and potentiometry), a custom-made miniature printed circuit board (PCB) powered by a 200 mAh Li-ion rechargeable battery that enables multiplexed decoding of sweat and wireless signal transduction to the host device was applied. The developed system was mounted on the epidermis and evaluated towards the real-time multiplexed determination of lactate (via amperometric transduction) and Na^+ , K^+ and pH (via potentiometric transduction) during stationary biking.

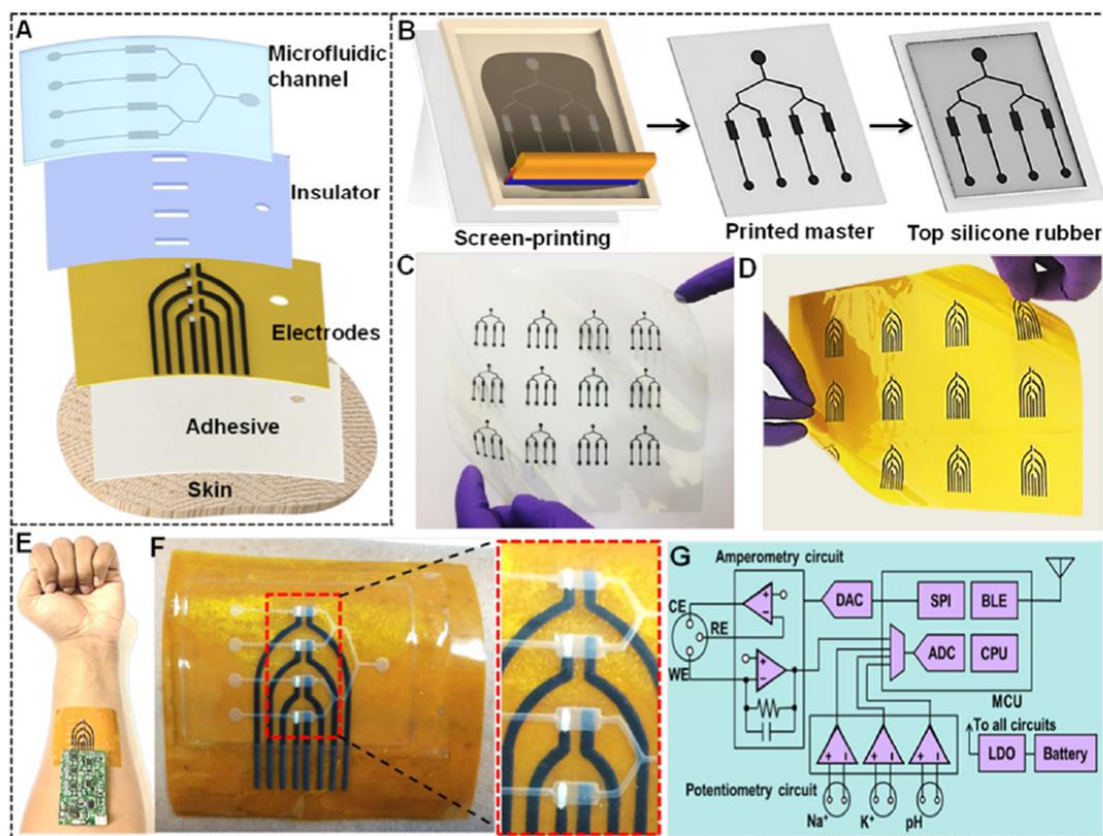


Figure 12. Overview of the fully printed microfluidic device proposed by Vinoth and colleagues. **(a)** Schematic representation of different layers of the microfluidic patch. **(b)** Schematic illustration of the fabrication of silicone rubber-based microfluidic channels from the screen-printed carbon master. The optical images showing an array of printed **(c)** carbon master and **(d)** multiarray electrodes. Images showing **(e)** the skin-interfaced, fully integrated microfluidic sensor and **(f)** the close-up part of multiarray electrode having four sensing chambers. **(g)** Scheme representing the layout of miniature PCB capable of multiplexed analysis and wireless data transmission. (Reprinted with permission from [42], Copyright (2020), American Chemical Society).

Table 1. Analytical features of 2D electrochemical (bio)sensors towards biomarkers determination

Biomarker	Electrode	Technique	Concentration range	LOD	Sample	Reference
A β ₁₋₄₀	rGO SPEs	DPV	10 fmol L ⁻¹ -10 pmol L ⁻¹	9.51 fmol L ⁻¹	Plasma	[43]
A β ₁₋₄₂	rGO SPEs	DPV	10 fmol L ⁻¹ -50 pmol L ⁻¹	8.65 fmol L ⁻¹	Plasma	[43]
NfL	MBs-SCPEs	Amperometry	10.0 pg L ⁻¹ -5000.0 pg L ⁻¹	3.0 pg mL ⁻¹	Plasma and brain tissue	[44]
EpCAM positive cancer cells	Apt/GNST/SiNP-IL/SPE	DPV	5 - 10 ⁷ cells mL ⁻¹	1 cell mL ⁻¹	Serum	[45]
Pyocyanin	AuNPs/rGO/SPCE	DPV	1.0 μ mol L ⁻¹ -100.0 pmol L ⁻¹	0.27 μ mol L ⁻¹	<i>P. aeruginosa</i> culture	[46]
Her-2	LSG-AuNS	SWV	0.1 ng mL ⁻¹ -200.0 ng mL ⁻¹	0.008 ng mL ⁻¹	Serum	[47]
Leptin	oPD/Streptavidin-HRP/Biotinylated α -Leptin/ α -leptin/DTSSP/SPGEs	SWV	0.1 ng mL ⁻¹ -20.0 ng mL ⁻¹	0.033 ng mL ⁻¹	Mouse blood serum	[48]
IgG	AgNPs/rGO/SPCE	SWV	1.0 pg mL ⁻¹ -50.0 pg mL ⁻¹ and 0.05 ng mL ⁻¹ -50.0 ng mL ⁻¹	0.086 pg mL ⁻¹	Serum	[37]
miR-21	ANSAm-DNA/SPCE	Coulometry	1.0 $\times 10^{-14}$ mol L ⁻¹ -1.0 $\times 10^{-8}$ mol L ⁻¹	17.0 fmol L ⁻¹	Urine	[36]
circRNA	AuNPs-SPME	DPV	1.0 pmol L ⁻¹ -100.0 nmol L ⁻¹	10.0 pmol L ⁻¹	Serum	[49]
PD-L1	SPCE	Amperometry	290 pg mL ⁻¹ -2500.0 pg mL ⁻¹	86 pg mL ⁻¹	Cancer cell lysates	[50]
HIF-1 α	SPCE	Amperometry	930 pg mL ⁻¹ -10,000 pg mL ⁻¹	279 pg mL ⁻¹	Cancer cell lysates	[50]
lncRNA biomarker MALAT1	Au NCs/MWCNT-NH ₂ -SPCE	DPV	1.0 $\times 10^{-14}$ mol L ⁻¹ -1.0 $\times 10^{-7}$ mol L ⁻¹	48.0 fmol L ⁻¹	Serum	[51]
miR-141	HRP-modified SPCE	Chronomperometry	1.0 $\times 10^{-12}$ mol L ⁻¹ -1.0 $\times 10^{-8}$ mol L ⁻¹	0.1 pmol L ⁻¹	Cohort of colorectal and	[52]

					breast cancer samples	
GPC3	RGO-H-CS/SPE	DPV	0.01 $\mu\text{g mL}^{-1}$ -10.0 $\mu\text{g mL}^{-1}$	7.9 ng mL^{-1}	Serum	[53]
miRNA-21	AuNPs/GQDs/GO/3SPCE	SWV	0.01 pmol L^{-1} -1000 pmol L^{-1}	0.04 fmol L^{-1}	Serum	[54]
miRNA-155	AuNPs/GQDs/GO/3SPCE	SWV	0.01 pmol L^{-1} -1000 pmol L^{-1}	0.33 fmol L^{-1}	Serum	[54]
miRNA-210	AuNPs/GQDs/GO/3SPCE	SWV	0.01 pmol L^{-1} -1000 pmol L^{-1}	0.28 fmol L^{-1}	Serum	[54]
cTnl	pAb ₂ -PBDENP/cTnl/mAb ₁ -BSA-SPCE	SWV	0.01 ng mL^{-1} -100 ng mL^{-1}	6.2 pg mL^{-1}	Serum	[55]
NIM	Fe ₃ O ₄ -3D GPE	SWV	0.8 $\mu\text{mol L}^{-1}$ -6 $\mu\text{mol L}^{-1}$	0.01 $\mu\text{mol L}^{-1}$	Serum and artificial urine	[56]
DOP	Fe ₃ O ₄ -3D GPE	SWV	0.5 $\mu\text{mol L}^{-1}$ -9 $\mu\text{mol L}^{-1}$	0.0023 $\mu\text{mol L}^{-1}$	Serum and artificial urine	[56]
UA	Fe ₃ O ₄ -3D GPE	SWV	0.7 $\mu\text{mol L}^{-1}$ -10 $\mu\text{mol L}^{-1}$	0.0034 $\mu\text{mol L}^{-1}$	Serum and artificial urine	[56]
Creatinine	Nafion/polyacrylic gel-Cu ²⁺ /cuprous oxide NPs/SPCE	CV/DPV/impedance/IoT	1 $\mu\text{mol L}^{-1}$ -2000 $\mu\text{mol L}^{-1}$	0.3 $\mu\text{mol L}^{-1}$	Artificial and in human saline	[57]
p53	AuNP-SPCE	LSV	2 nmol L^{-1} -50 mol L^{-1}	0.05 nmol L^{-1}	Plasma	[58]
Uric acid	SPCE-MNC	DPV	0-70 $\mu\text{mol L}^{-1}$	1.8 $\mu\text{mol L}^{-1}$	Artificial sweat	[59]
17 β -estradiol	SPCE-MNC	DPV	0-3 $\mu\text{mol L}^{-1}$	0.27 $\mu\text{mol L}^{-1}$	Artificial sweat	[59]
NGAL	Dual-SPCE	LSV	0.15 ng mL^{-1} -2.0 ng mL^{-1}	0.096 ng mL^{-1}	Urine	[60]
HER2	HOOC-MBs/SPCE	LSV	5.0 ng mL^{-1} -50 ng mL^{-1} and 50 ng mL^{-1} -100 ng mL^{-1}	2.8 ng mL^{-1}	Serum	[61]

miR-21	rGO/Au/SPE	DPV	$1.0 \times 10^{-12} \text{ mol L}^{-1}$ - $1.0 \times 10^{-4} \text{ mol L}^{-1}$	1.0 pmol L^{-1}	Saliva	[62]
RANKL	Neu-MBs/SPdCEs	Amperometry	0.0 - $1,000 \text{ pg mL}^{-1}$	2.6 pg mL^{-1}	Serum	[63]
TNF	Neu-MBs/SPdCEs	Amperometry	0.0 - $1,000 \text{ pg mL}^{-1}$	3.0 pg mL^{-1}	Serum	[63]
Tau protein	3D-Au-PAMAM-p-ABA-SPCE	Amperometry	6.0 - $5,000 \text{ pg mL}^{-1}$	1.7 pg mL^{-1}	Plasma and brain tissue extracts	[64]
HOTAIR RNA	SPE-Au	Chronomperometry	1 fmol L^{-1} - 1 nmol L^{-1}	1.0 fmol L^{-1}	Ovarian Cancer Cell Lines and plasma	[65]
Gal-3	SPCE	Chronomperometry	$2.8 \times 10^{-2} \text{ ng mL}^{-1}$ - 5 ng mL^{-1}	8.3 pg mL^{-1}	Plasma	[66]
PSA	ce-MoS ₂ /AgNR/SPE	CV	0.1 ng mL^{-1} - 1000 ng mL^{-1}	0.051 ng mL^{-1}	---	[67]
p53	SPCEs/PEI/NPs	DPV	1.0 pg mL^{-1} - $10 \times 10^3 \text{ pg mL}^{-1}$	5.0 fg mL^{-1}	Fetal bovine serum, cell lysate and saliva	[68]
CA19-9	SPCE/CB-PEI/CB-PAA	DPV	0.01 U mL^{-1} - 40 U mL^{-1}	0.07 U mL^{-1}	Serum and cell lysate	[69]
serpin A12	MCH/thiolated aptamer/FLGMs/SPCE	DPV	0.039 ng mL^{-1} - 10 ng mL^{-1}	0.02 ng mL^{-1}	Plasma	[70]
miR-21	His-Tag-Isolation-MBs/SPCE	Amperometry	3.0 nmol L^{-1} - 100 nmol L^{-1}	0.91 nmol L^{-1}	RNA _t extracted from epithelial non-tumorigenic and adenocarcinoma breast cells	[71]

A β ₁₋₄₂	Au film Graphene/rGO-SPE	DPV	11 pmol L ⁻¹ -55nmol L ⁻¹	2.398 pmol L ⁻¹	Human and mice plasmas	[72]
Insulin	MWNT-QD modified SPE array	SWV	100 pmol L ⁻¹ -5000pmol L ⁻¹	100 pmol L ⁻¹	---	[73]
CYFRA 21-1	CoZnFeONPs	Amperometry	3.9 fg mL ⁻¹ -1000 fg mL ⁻¹	0.19 fg mL ⁻¹	Serum samples from healthy and prostate cancer patients	[38]
PSA	MIP-SPE	EIS	0.01 ng mL ⁻¹ -100 ng mL ⁻¹	5.4 pg mL ⁻¹	Serum and urine	[74]
Myo	MIP-SPE	EIS	1 nm mL ⁻¹ -20000 ng mL ⁻¹	0.83 ng mL ⁻¹	Serum and urine	[74]
INO	(PNP-CS) ₂ -SPCE	SWV	2 μ mol L ⁻¹ -90 μ mol L ⁻¹	0.3 μ mol L ⁻¹	Serum (from normal and myocardial infarction patients) and dietary supplements	[75]
CA19-9	SPIDE/CNO-GO	EIS	0.3 U mL ⁻¹ -100 U mL ⁻¹	0.12 U mL ⁻¹	Whole-cell lysates of colorectal adenocarcinoma	[76]
CEA	NG-THI-AuNPs modified paper electrode	DPV	0.01 ng mL ⁻¹ -500 ng mL ⁻¹	2.0 pg mL ⁻¹	Serum	[77]
NSE	PB-PEDOT-AuNPs modified paper electrode	DPV	0.05 ng mL ⁻¹ -500 ng mL ⁻¹	10.0 pg mL ⁻¹	Serum	[77]

CXCL7	IgG-MWCNTs/SPCE	DPV	0.5 pg mL ⁻¹ -600 pg mL ⁻¹	0.1 pg mL ⁻¹	Serum samples from patients with rheumatoid arthritis	[78]
IL-13R α 2	SPdCEs	Amperometry	3.4 ng mL ⁻¹ -100 ng mL ⁻¹	1.03 ng mL ⁻¹	Serum and paraffined-embedded tissues from colorectal cancer (CRC) patients	[79]
E-CDH	SPdCEs	Amperometry	0.9 ng mL ⁻¹ -25 ng mL ⁻¹	3.45 ng mL ⁻¹	Serum and paraffined-embedded tissues from colorectal cancer (CRC) patients	[79]
AFP	PEI-AuNPs/SPCE	SWV	0.25 ng mL ⁻¹ -10 ng mL ⁻¹	1.7 fg mL ⁻¹	Serum	[80]
CEA	PEI-AuNPs/SPCE	SWV	0.25 ng mL ⁻¹ -10 ng mL ⁻¹	1.6 fg mL ⁻¹	Serum	[80]
PSA	PEI-AuNPs/SPCE	SWV	0.25 ng mL ⁻¹ -10 ng mL ⁻¹	0.9 fg mL ⁻¹	Serum	[80]
IL-8	PEI-AuNPs/SPCE	SWV	0.50 pg mL ⁻¹ -100 pg mL ⁻¹	1.0 fg mL ⁻¹	Serum	[80]
PSA	CASPE-MFD	Chronoamperometry	0.001 ng mL ⁻¹ -10 ng mL ⁻¹	0.84 Pg mL ⁻¹	Serum	[81]
8-OHdG	SPE-Gr	LSV	3.0 $\times 10^{-7}$ mol L ⁻¹ -1.0 $\times 10^{-4}$ mol L ⁻¹	90 nmol L ⁻¹	Saliva	[82]
p24-HIV	GQD-SPE	CV	0.93 ng mL ⁻¹ -93 μ g mL ⁻¹	51.7 pg mL ⁻¹	Serum	

A β ₁₋₄₀ e A β ₁₋₄₂: Alzheimer's disease biomarkers; rGO: reduced graphene oxide; NFL: neurofilament light chain, an Alzheimer's disease biomarker; MBs: magnetic microbeads; Apt: aptamer; GNST: gold nanostar structures; SiNP: porous silica nanoparticles; IL: ionic liquid; CTCs: DPV:

differential pulse voltammetry; SCPes: screen-printed carbon electrodes; EID50: ; Her-2: human epidermal growth factor receptor 2; SWV: Square-wave voltammetry; LSG-AuNS: nanostructured gold modified laser-scribed graphene-based electrode; oPD: o-phenylenediamine; SPGEs: screen-printed gold electrodes; HRP: horseradish peroxidase; DTSSP: sulfosuccinimidyl propionate; IgG: human immunoglobulin G; miR-21: urinary microRNA; ANSA_m: 4-amino-3-hydroxy-1-naphthalene sulfonic acid; circRNA: circular RNA from hepatocellular cancer; SPME: screen-printed magnetic electrode; PD-L1: programmed death ligand 1 protein; HIF-1 α : hypoxia-inducible factor 1 alpha protein; Au NCs/MWCNT-NH₂: gold nanocage coupled with an amidated multi-walled carbon nanotube; lncRNA biomarker MALAT1: Long non-coding RNA biomarker for the screening of non-small cell lung cancer; miR-141: microRNA associated to cancers such as colorectal cancer (CRC) and breast cancer (BC); GPC3: glypican-3; cTnl: cardiac troponin I; PBDENPs: Prussian blue-doped PAMAM dendrimer nanospheres; 3D GPE: graphene paste electrodes; IoT: Internet of Things; p53: protein biomarker for Alzheimer's disease; LSV: linear sweep voltammetry; NGAL: neutrophil gelatinase associated lipocalin; HER2: Human Epidermal growth factor Receptor 2; HOOC-MBs: biomodified carboxylic acid functionalized magnetic beads; RANKL: Receptor Activator of Nuclear Factor- κ B related to breast cancer (BC); TNF: Tumor Necrosis Factor alpha related to breast cancer (BC); Neu-MBs: neutravidin-functionalized magnetic microbeads; SPdCEs: dual screen-printed carbon electrodes; 3D-Au-PAMAM: gold nanoparticles-poly(amidoamine) dendrimer nanocomposite; *p*-ABA: p-aminobenzoic acid; Tau protein: hallmark of Alzheimer's disease; HOTAIR RNA: Long non-coding RNA HOX transcript antisense intergenic; SPE-Au: screen-printed gold electrode; Gal-3: galectin-3, a β -galactosidase-binding lectin that acts as mediator of heart failure (HF); PSA: prostate-specific antigen; ce-MoS₂: chemical exfoliated MoS₂ nanosheets; AgNR: Ag nanorods; CV: cyclic voltammetry; NPs: carboxylated NiFe₂O₄ nanoparticles; PEI: polyethyleneimine; CA19-9: cancer marker carbohydrate antigen 19-9; CB-PEI: carbon black- polyethyleneimine; CB-PAA: carbon black-polyacrylic acid; serpin A12: Type 2 diabetes biomarker; MCH: 6-mercapto-1-hexanol; FLGMs: flower-like gold microstructures; His-Tag-Isolation-MBs: commercial His-Tag-Zinc finger protein conjugated to magnetic beads; RNA_t: total RNA; A β ₁₋₄₂: beta-amyloid biomarker in Alzheimer's disease; MWNT-QD: Quantum dot decorated multi-walled carbon nanotube; CYFRA 21-1: protein biomarker in different types of cancer; CoZnFeONPs: Co_{0.25}Zn_{0.75}Fe₂O₄ nanoparticles; Myo: myoglobin; EIS: electrochemical impedance spectroscopy; MIP: molecularly imprinted polymer; INO: inosine; PNP: purine nucleoside phosphorylase; CS: chitosan; CA19-9: pancreatic cancer biomarker; SPIDE: screen-printed interdigitated electrodes; CNO: carbon nano-onion; GO: graphene oxide; NG-THI-AuNPs: amino functional graphene-thionin- gold nanoparticles; PB-PEDOT-AuNPs: prussian blue-poly (3,4- ethylenedioxythiophene)-gold nanoparticles; CXCL7: chemokine (C-X-C motif) ligand autoimmune biomarker; IL-13R α 2: interleukin-13 receptor α 2; E-CDH: E-cadherin; AFP: alpha fetoprotein; CEA: carcinoembryonic antigen; IL-8 interleukin-8; CASPE-MFD: screen-printed electrode-based microfluidic device; 8-OHdG: 8-hydroxy-2'-deoxyguanosine; p24-HIV: protein monitored in the early diagnosis of HIV; GQD: graphene quantum dots.

3. Conclusions and Perspectives

Most biomarker analysis methods are based on laboratory analytical techniques that commonly require expensive and bulky equipment, including chromatographic or spectrometric methods, among others. In this sense, miniaturized analytical systems present special advantages such as portability and low cost and can be used for applications outside the laboratory environment to overcome the disadvantages of conventional analytical procedures, reduce total analytical time, or increase efficiency.

As presented in this book chapter, miniaturized devices based on electrochemical systems have evolved rapidly on monitoring of biomarkers due to several aspects as simplicity, high sensitivity and selectivity, reduced power requirements, and good compatibility with biological samples. In addition, its compatibility with advanced microfabrication technologies allows the replacement of conventional electrochemical cells and electrodes with easy-to-use miniaturized electrochemical systems.

The great advantage of miniaturized electrochemical devices is their versatility of construction. Those based mainly on 2D printing methods, are produced using low cost techniques, easily scalable and with different recyclable materials. We present along with the text the great potential of these sensors for detecting biomarkers and, in recent years, they have also been widely applied in various fields, including health, food safety and environmental monitoring.

Finally, 2D printing strategies applied to the development of miniaturized electrochemical systems are technologies that are fully suited to the precepts of analytical chemistry. The integration between devices built on 2D parts and electrochemical systems is one of the most promising trends in today's electroanalytical and considering the exponential growth of publications these parts fabrication strategies will remain popular soon.

Acknowledgment

The authors are grateful to CNPq (402943/2016-3, 408309/2018-0, 303338/2019-9, 309803/2020-9, 311290/2020-5), CAPES (001 and Pandemias 8887.504861/2020-00), FAPESP (2017/21097-3), and FAPEMIG (APQ-00083-21) for the financial support.

References

- [1] F. Navarrete, F. Sala, M.S. Garc, Biomarkers in Psychiatry : Concept , De finition , Types and Relevance to the Clinical Reality, *Front. Psychiatry*. 11 (2020) 1–14. <https://doi.org/10.3389/fpsyt.2020.00432>.
- [2] M.J. Pletcher, M. Pignone, Evaluating the Clinical Utility of a Biomarker: A Review of Methods for Estimating Health Impact, *Circulation*. 123 (2011) 1116–1124. <https://doi.org/10.1161/CIRCULATIONAHA.110.943860.Evaluating>.
- [3] J.K. Aronson, R.E. Ferner, Biomarkers—a general review, *Curr. Protoc. Pharmacol.* 2017 (2017) 9.23.1-9.23.17. <https://doi.org/10.1002/cpph.19>.
- [4] K. Strimbu, J.A. Tavel, What are biomarkers?, *Curr. Opin. HIV AIDS*. 5 (2010) 463–466. <https://doi.org/10.1097/COH.0b013e32833ed177>.
- [5] S.A. Byrnes, B.H. Weigl, Selecting analytical biomarkers for diagnostic applications: a first principles approach, *Expert Rev. Mol. Diagn.* 18 (2018) 19–26. <https://doi.org/10.1080/14737159.2018.1412258>.
- [6] D.R. Reyes, D. Iossifidis, P.A. Auroux, A. Manz, Micro total analysis systems. 1. Introduction, theory, and technology, *Anal. Chem.* 74 (2002) 2623–2636. <https://doi.org/10.1021/ac0202435>.

- [7] Á. Ríos, M. Zougagh, M. Avila, Miniaturization through lab-on-a-chip: Utopia or reality for routine laboratories? A review, *Anal. Chim. Acta.* 740 (2012) 1–11. <https://doi.org/10.1016/j.aca.2012.06.024>.
- [8] C.W. Foster, R.O. Kadara, C.E. Banks, *Screen-Printing Electrochemical Architectures*, 2016.
- [9] S.K. Tuteja, C. Ormsby, S. Neethirajan, Noninvasive Label-Free Detection of Cortisol and Lactate Using Graphene Embedded Screen-Printed Electrode, *Nano-Micro Lett.* 10 (2018) 1–10. <https://doi.org/10.1007/s40820-018-0193-5>.
- [10] A.N. Nordin, A.A. Zainuddin, R.A. Rahim, I. Voiculescu, W.C. Mak, Screen Printed Electromechanical Micro-total Analysis System (μ tas) for Sensitive and Rapid Detection of Infectious Diseases, *Procedia Technol.* 27 (2017) 100–101. <https://doi.org/10.1016/J.PROTCY.2017.04.043>.
- [11] R.A.S. Couto, J.L.F.C. Lima, M.B. Quinaz, Recent developments, characteristics and potential applications of screen-printed electrodes in pharmaceutical and biological analysis, *Talanta.* 146 (2016) 801–814. <https://doi.org/https://doi.org/10.1016/j.talanta.2015.06.011>.
- [12] J.P. Mensing, T. Lomas, A. Tuantranont, 2D and 3D printing for graphene based supercapacitors and batteries: A review, *Sustain. Mater. Technol.* 25 (2020) e00190. <https://doi.org/https://doi.org/10.1016/j.susmat.2020.e00190>.
- [13] G. Hu, J. Kang, L.W.T. Ng, X. Zhu, R.C.T. Howe, C.G. Jones, M.C. Hersam, T. Hasan, Functional inks and printing of two-dimensional materials, *Chem. Soc. Rev.* 47 (2018) 3265–3300. <https://doi.org/10.1039/C8CS00084K>.
- [14] J.R. Windmiller, A.J. Bhandodkar, S. Parkhomovsky, J. Wang, Stamp transfer electrodes for electrochemical sensing on non-planar and oversized surfaces, *Analyst.* 137 (2012) 1570–1575. <https://doi.org/10.1039/C2AN35041F>.
- [15] I.A. de Araujo Andreotti, L.O. Orzari, J.R. Camargo, R.C. Faria, L.H. Marcolino-Junior, M.F. Bergamini, A. Gatti, B.C. Janegitz, Disposable and flexible electrochemical sensor made by recyclable material and low cost conductive ink, *J. Electroanal. Chem.* 840 (2019) 109–116. <https://doi.org/https://doi.org/10.1016/j.jelechem.2019.03.059>.
- [16] A.S. Afonso, C. V Uliana, D.H. Martucci, R.C. Faria, Simple and rapid fabrication of disposable carbon-based electrochemical cells using an electronic craft cutter for sensor and biosensor applications, *Talanta.* 146 (2016) 381–387. <https://doi.org/https://doi.org/10.1016/j.talanta.2015.09.002>.
- [17] S. Cinti, V. Mazzaracchio, I. Cacciotti, D. Moscone, F. Arduini, Carbon Black-Modified Electrodes Screen-Printed onto Paper Towel, Waxed Paper and Parafilm M®, *Sensors* . 17 (2017). <https://doi.org/10.3390/s17102267>.
- [18] E. Noviana, C.P. McCord, K.M. Clark, I. Jang, C.S. Henry, Electrochemical paper-based devices: sensing approaches and progress toward practical applications, *Lab Chip.* 20 (2020) 9–34. <https://doi.org/10.1039/C9LC00903E>.
- [19] A.A. Dias, T.M.G. Cardoso, C.L.S. Chagas, V.X.G. Oliveira, R.A.A. Munoz, C.S. Henry, M.H.P. Santana, T.R.L.C. Paixão, W.K.T. Coltro, Detection of Analgesics and Sedation Drugs in Whiskey Using Electrochemical Paper-based Analytical Devices, *Electroanalysis.* 30 (2018) 2250–2257. <https://doi.org/https://doi.org/10.1002/elan.201800308>.
- [20] T.F. Yi, H.M.K. Sari, X. Li, F. Wang, Y.R. Zhu, J. Hu, J. Zhang, X. Li, A review of niobium oxides based nanocomposites for lithium-ion batteries, sodium-ion batteries and supercapacitors, *Nano Energy.* 85 (2021) 105955. <https://doi.org/10.1016/j.nanoen.2021.105955>.
- [21] J.R. Camargo, L.O. Orzari, D.A.G. Araújo, P.R. de Oliveira, C. Kalinke, D.P.

- Rocha, A. Luiz dos Santos, R.M. Takeuchi, R.A.A. Munoz, J.A. Bonacin, B.C. Janegitz, Development of conductive inks for electrochemical sensors and biosensors, *Microchem. J.* 164 (2021) 105998. <https://doi.org/https://doi.org/10.1016/j.microc.2021.105998>.
- [22] K. Parvez, R. Worsley, A. Alieva, A. Felten, C. Casiraghi, Water-based and inkjet printable inks made by electrochemically exfoliated graphene, *Carbon N. Y.* 149 (2019) 213–221. <https://doi.org/https://doi.org/10.1016/j.carbon.2019.04.047>.
- [23] H. Wei, J.-J. Sun, Y. Xie, C.-G. Lin, Y.-M. Wang, W.-H. Yin, G.-N. Chen, Enhanced electrochemical performance at screen-printed carbon electrodes by a new pretreating procedure, *Anal. Chim. Acta.* 588 (2007) 297–303. <https://doi.org/https://doi.org/10.1016/j.aca.2007.02.006>.
- [24] P. Labroo, Y. Cui, Graphene nano-ink biosensor arrays on a microfluidic paper for multiplexed detection of metabolites, *Anal. Chim. Acta.* 813 (2014) 90–96. <https://doi.org/https://doi.org/10.1016/j.aca.2014.01.024>.
- [25] J.-W. Han, B. Kim, J. Li, M. Meyyappan, Carbon nanotube ink for writing on cellulose paper, *Mater. Res. Bull.* 50 (2014) 249–253. <https://doi.org/https://doi.org/10.1016/j.materresbull.2013.10.048>.
- [26] Y. Sekertekin, I. Bozyel, D. Gokcen, A Flexible and Low-Cost Tactile Sensor Produced by Screen Printing of Carbon Black/PVA Composite on Cellulose Paper, *Sensors* . 20 (2020). <https://doi.org/10.3390/s20102908>.
- [27] S.M.V. dos Santos, P.R. Oliveira, M.C. Oliveira, M.F. Bergamini, L.H. Marcolino-Jr, Eletrodos impressos construídos por serigrafia utilizando negro de fumo como material condutor, *Rev. Virtual Química.* 9 (2017).
- [28] M. Pavithra, S. Muruganand, C. Parthiban, Development of novel paper based electrochemical immunosensor with self-made gold nanoparticle ink and quinone derivate for highly sensitive carcinoembryonic antigen, *Sensors Actuators B Chem.* 257 (2018) 496–503. <https://doi.org/https://doi.org/10.1016/j.snb.2017.10.177>.
- [29] I.J. Fernandes, A.F. Aroche, A. Schuck, P. Lamberty, C.R. Peter, W. Hasenkamp, T.L.A.C. Rocha, Silver nanoparticle conductive inks: synthesis, characterization, and fabrication of inkjet-printed flexible electrodes, *Sci. Rep.* 10 (2020) 8878. <https://doi.org/10.1038/s41598-020-65698-3>.
- [30] A. Abellán-Llobregat, I. Jeerapan, A. Bandodkar, L. Vidal, A. Canals, J. Wang, E. Morallón, A stretchable and screen-printed electrochemical sensor for glucose determination in human perspiration, *Biosens. Bioelectron.* 91 (2017) 885–891. <https://doi.org/https://doi.org/10.1016/j.bios.2017.01.058>.
- [31] W. Li, M. Chen, Synthesis of stable ultra-small Cu nanoparticles for direct writing flexible electronics, *Appl. Surf. Sci.* 290 (2014) 240–245. <https://doi.org/https://doi.org/10.1016/j.apsusc.2013.11.057>.
- [32] S. Bi, W. Dong, B. Lan, H. Zhao, L. Hou, L. Zhu, Y. Xu, Y. Lu, Flexible carbonic pen ink/carbon fiber paper composites for multifunctional switch-type sensors, *Compos. Part A Appl. Sci. Manuf.* 124 (2019) 105452. <https://doi.org/https://doi.org/10.1016/j.compositesa.2019.05.020>.
- [33] D.A.G. Araújo, J.R. Camargo, L.A. Pradela-Filho, A.P. Lima, R.A.A. Muñoz, R.M. Takeuchi, B.C. Janegitz, A.L. Santos, A lab-made screen-printed electrode as a platform to study the effect of the size and functionalization of carbon nanotubes on the voltammetric determination of caffeic acid, *Microchem. J.* 158 (2020) 105297. <https://doi.org/https://doi.org/10.1016/j.microc.2020.105297>.
- [34] X. Liu, Y. Yao, Y. Ying, J. Ping, Recent advances in nanomaterial-enabled

- screen-printed electrochemical sensors for heavy metal detection, *TrAC Trends Anal. Chem.* 115 (2019) 187–202.
<https://doi.org/https://doi.org/10.1016/j.trac.2019.03.021>.
- [35] M. Trojanowicz, Impact of nanotechnology on design of advanced screen-printed electrodes for different analytical applications, *TrAC Trends Anal. Chem.* 84 (2016) 22–47. <https://doi.org/https://doi.org/10.1016/j.trac.2016.03.027>.
- [36] D.A. Smith, K. Simpson, M. Lo Cicero, L.J. Newbury, P. Nicholas, D.J. Fraser, N. Caiger, J.E. Redman, T. Bowen, Detection of urinary microRNA biomarkers using diazo sulfonamide-modified screen printed carbon electrodes, *RSC Adv.* 11 (2021) 18832–18839. <https://doi.org/10.1039/D0RA09874D>.
- [37] S. Chanarsa, J. Jakmunee, K. Ounnunkad, A Bifunctional Nanosilver-Reduced Graphene Oxide Nanocomposite for Label-Free Electrochemical Immunosensing, *Front. Chem.* 9 (2021) 245.
<https://www.frontiersin.org/article/10.3389/fchem.2021.631571>.
- [38] C.A. Proença, T.A. Baldo, T.A. Freitas, E.M. Materón, A. Wong, A.A. Durán, M.E. Melendez, G. Zambrano, R.C. Faria, Novel enzyme-free immunomagnetic microfluidic device based on $\text{Co}_0.25\text{Zn}_0.75\text{Fe}_2\text{O}_4$ for cancer biomarker detection, *Anal. Chim. Acta.* 1071 (2019) 59–69.
<https://doi.org/https://doi.org/10.1016/j.aca.2019.04.047>.
- [39] T.R. de Oliveira, C.R. Erbereli, P.R. Manzine, T.N.C. Magalhães, M.L.F. Balthazar, M.R. Cominetti, R.C. Faria, Early Diagnosis of Alzheimer’s Disease in Blood Using a Disposable Electrochemical Microfluidic Platform, *ACS Sensors.* 5 (2020) 1010–1019. <https://doi.org/10.1021/acssensors.9b02463>.
- [40] E.L. Fava, T.A. Silva, T.M.D. Prado, F.C.D. Moraes, R.C. Faria, O. Fatibello-Filho, Electrochemical paper-based microfluidic device for high throughput multiplexed analysis, *Talanta.* 203 (2019).
<https://doi.org/10.1016/j.talanta.2019.05.081>.
- [41] E.L. Fava, T. Martimiano do Prado, T. Almeida Silva, F. Cruz de Moraes, R. Censi Faria, O. Fatibello-Filho, New Disposable Electrochemical Paper-based Microfluidic Device with Multiplexed Electrodes for Biomarkers Determination in Urine Sample, *Electroanalysis.* 32 (2020) 1075–1083.
<https://doi.org/https://doi.org/10.1002/elan.201900641>.
- [42] R. Vinoth, T. Nakagawa, J. Mathiyarasu, A.M.V. Mohan, Fully Printed Wearable Microfluidic Devices for High-Throughput Sweat Sampling and Multiplexed Electrochemical Analysis, *ACS Sensors.* 6 (2021) 1174–1186.
<https://doi.org/10.1021/acssensors.0c02446>.
- [43] J. Sethi, A. Suhail, M. Safarzadeh, A. Sattar, Y. Wei, G. Pan, NH_2 linker for femtomolar label-free detection with reduced graphene oxide screen-printed electrodes, *Carbon N. Y.* 179 (2021) 514–522.
<https://doi.org/https://doi.org/10.1016/j.carbon.2021.04.074>.
- [44] A. Valverde, A. Montero-Calle, R. Barderas, M. Calero, P. Yáñez-Sedeño, S. Campuzano, J.M. Pingarrón, Electrochemical immunoplatfom to unravel neurodegeneration and Alzheimer’s disease through the determination of neurofilament light protein, *Electrochim. Acta.* 371 (2021) 137815.
<https://doi.org/https://doi.org/10.1016/j.electacta.2021.137815>.
- [45] A. Bagheri Hashkavayi, B.S. Cha, S.H. Hwang, J. Kim, K.S. Park, Highly sensitive electrochemical detection of circulating EpCAM-positive tumor cells using a dual signal amplification strategy, *Sensors Actuators B Chem.* 343 (2021) 130087. <https://doi.org/https://doi.org/10.1016/j.snb.2021.130087>.
- [46] J.I.A. Rashid, V. Kannan, M.H. Ahmad, A.A. Mon, S. Taufik, A. Miskon, K.K.

- Ong, N.A. Yusof, An electrochemical sensor based on gold nanoparticles-functionalized reduced graphene oxide screen printed electrode for the detection of pyocyanin biomarker in *Pseudomonas aeruginosa* infection, *Mater. Sci. Eng. C*. 120 (2021) 111625.
<https://doi.org/https://doi.org/10.1016/j.msec.2020.111625>.
- [47] S. Rauf, A.A. Lahcen, A. Aljedaibi, T. Beduk, J. Ilton de Oliveira Filho, K.N. Salama, Gold nanostructured laser-scribed graphene: A new electrochemical biosensing platform for potential point-of-care testing of disease biomarkers, *Biosens. Bioelectron.* 180 (2021) 113116.
<https://doi.org/https://doi.org/10.1016/j.bios.2021.113116>.
- [48] R. Sung, Y.S. Heo, Sandwich ELISA-Based Electrochemical Biosensor for Leptin in Control and Diet-Induced Obesity Mouse Model, *Biosens.* . 11 (2021).
<https://doi.org/10.3390/bios11010007>.
- [49] B. Zhang, Y. Liang, L. Bo, M. Chen, B. Huang, Q. Cao, J. Wei, T. Li, X. Cai, X. Ye, A PCR-free screen-printed magnetic electrode for the detection of circular RNA from hepatocellular cancer based on a back-splice junction, *RSC Adv.* 11 (2021) 17769–17774. <https://doi.org/10.1039/D1RA01033F>.
- [50] C. Muñoz-San Martín, M. Gamella, M. Pedrero, A. Montero-Calle, V. Pérez-Ginés, J. Camps, M. Arenas, R. Barderas, J.M. Pingarrón, S. Campuzano, Anticipating metastasis through electrochemical immunosensing of tumor hypoxia biomarkers, *Anal. Bioanal. Chem.* (2021).
<https://doi.org/10.1007/s00216-021-03240-8>.
- [51] M. Chen, D. Wu, S. Tu, C. Yang, D. Chen, Y. Xu, A novel biosensor for the ultrasensitive detection of the lncRNA biomarker MALAT1 in non-small cell lung cancer, *Sci. Rep.* 11 (2021) 3666. <https://doi.org/10.1038/s41598-021-83244-7>.
- [52] W.-H. Leung, C.-C. Pang, S.-N. Pang, S.-X. Weng, Y.-L. Lin, Y.-E. Chiou, S.-T. Pang, W.-H. Weng, High-Sensitivity Dual-Probe Detection of Urinary miR-141 in Cancer Patients via a Modified Screen-Printed Carbon Electrode-Based Electrochemical Biosensor, *Sensors* . 21 (2021).
<https://doi.org/10.3390/s21093183>.
- [53] M. Chen, H. Li, X. Su, R. Wu, H. Feng, X. Shi, J. Liang, J. Chen, G. Li, Label-free electrochemical aptasensor based on reduced graphene oxide–hemin–chitosan nanocomposite for the determination of glypican-3, *New J. Chem.* 45 (2021) 8608–8618. <https://doi.org/10.1039/D1NJ00633A>.
- [54] C. Pothipor, J. Jakmunee, S. Bamrungsap, K. Ounnunkad, An electrochemical biosensor for simultaneous detection of breast cancer clinically related microRNAs based on a gold nanoparticles/graphene quantum dots/graphene oxide film, *Analyst.* 146 (2021) 4000–4009.
<https://doi.org/10.1039/D1AN00436K>.
- [55] F. Ma, G. Ge, Y. Fang, E. Ni, Y. Su, F. Cai, H. Xie, Prussian blue-doped PAMAM dendrimer nanospheres for electrochemical immunoassay of human plasma cardiac troponin I without enzymatic amplification, *New J. Chem.* 45 (2021) 9621–9628. <https://doi.org/10.1039/D1NJ01506K>.
- [56] E.M. Materon, A. Wong, L.M. Gomes, G. Ibáñez-Redín, N. Joshi, O.N. Oliveira, R.C. Faria, Combining 3D printing and screen-printing in miniaturized, disposable sensors with carbon paste electrodes, *J. Mater. Chem. C*. 9 (2021) 5633–5642. <https://doi.org/10.1039/D1TC01557E>.
- [57] S. Kalasin, P. Sangnuang, P. Khownarumit, I.M. Tang, W. Surareungchai, Salivary Creatinine Detection Using a Cu(I)/Cu(II) Catalyst Layer of a

- Supercapacitive Hybrid Sensor: A Wireless IoT Device To Monitor Kidney Diseases for Remote Medical Mobility, *ACS Biomater. Sci. Eng.* 6 (2020) 5895–5910. <https://doi.org/10.1021/acsbiomaterials.0c00864>.
- [58] O. Amor-Gutiérrez, E. Costa-Rama, N. Arce-Varas, C. Martínez-Rodríguez, A. Novelli, M.T. Fernández-Sánchez, A. Costa-García, Competitive electrochemical immunosensor for the detection of unfolded p53 protein in blood as biomarker for Alzheimer's disease, *Anal. Chim. Acta.* 1093 (2020) 28–34. <https://doi.org/https://doi.org/10.1016/j.aca.2019.09.042>.
- [59] R.R. Silva, P.A. Raymundo-Pereira, A.M. Campos, D. Wilson, C.G. Otoni, H.S. Barud, C.A.R. Costa, R.R. Domenegueti, D.T. Balogh, S.J.L. Ribeiro, O.N. Oliveira Jr., Microbial nanocellulose adherent to human skin used in electrochemical sensors to detect metal ions and biomarkers in sweat, *Talanta.* 218 (2020) 121153. <https://doi.org/https://doi.org/10.1016/j.talanta.2020.121153>.
- [60] M.M.P.S. Neves, H.P.A. Nouws, A. Santos-Silva, C. Delerue-Matos, Neutrophil gelatinase-associated lipocalin detection using a sensitive electrochemical immunosensing approach, *Sensors Actuators B Chem.* 304 (2020) 127285. <https://doi.org/https://doi.org/10.1016/j.snb.2019.127285>.
- [61] M. Freitas, H.P.A. Nouws, E. Keating, C. Delerue-Matos, High-performance electrochemical immunomagnetic assay for breast cancer analysis, *Sensors Actuators B Chem.* 308 (2020) 127667. <https://doi.org/https://doi.org/10.1016/j.snb.2020.127667>.
- [62] S. Shin Low, Y. Pan, D. Ji, Y. Li, Y. Lu, Y. He, Q. Chen, Q. Liu, Smartphone-based portable electrochemical biosensing system for detection of circulating microRNA-21 in saliva as a proof-of-concept, *Sensors Actuators B Chem.* 308 (2020) 127718. <https://doi.org/https://doi.org/10.1016/j.snb.2020.127718>.
- [63] A. Valverde, V. Serafín, J. Garoz, A. Montero-Calle, A. González-Cortés, M. Arenas, J. Camps, R. Barderas, P. Yáñez-Sedeño, S. Campuzano, J.M. Pingarrón, Electrochemical immunoplatform to improve the reliability of breast cancer diagnosis through the simultaneous determination of RANKL and TNF in serum, *Sensors Actuators B Chem.* 314 (2020) 128096. <https://doi.org/https://doi.org/10.1016/j.snb.2020.128096>.
- [64] C.A. Razzino, V. Serafín, M. Gamella, M. Pedrero, A. Montero-Calle, R. Barderas, M. Calero, A.O. Lobo, P. Yáñez-Sedeño, S. Campuzano, J.M. Pingarrón, An electrochemical immunosensor using gold nanoparticles-PAMAM-nanostructured screen-printed carbon electrodes for tau protein determination in plasma and brain tissues from Alzheimer patients, *Biosens. Bioelectron.* 163 (2020) 112238. <https://doi.org/https://doi.org/10.1016/j.bios.2020.112238>.
- [65] N. Soda, M. Umer, N. Kashaninejad, S. Kasetsirikul, R. Kline, C. Salomon, N.-T. Nguyen, M.J.A. Shiddiky, PCR-Free Detection of Long Non-Coding HOTAIR RNA in Ovarian Cancer Cell Lines and Plasma Samples, *Cancers* . 12 (2020). <https://doi.org/10.3390/cancers12082233>.
- [66] S. V Piguillem, M. Gamella, P. García de Frutos, M. Batlle, P. Yáñez-Sedeño, G.A. Messina, M.A. Fernández-Baldo, S. Campuzano, M. Pedrero, J.M. Pingarrón, Easily Multiplexable Immunoplatform to Assist Heart Failure Diagnosis through Amperometric Determination of Galectin-3, *Electroanalysis.* 32 (2020) 2775–2785. <https://doi.org/https://doi.org/10.1002/elan.202060323>.
- [67] J.-C. Gui, L. Han, C.-X. Du, X.-N. Yu, K. Hu, L.-H. Li, An efficient label-free immunosensor based on ce-MoS₂/AgNR composites and screen-printed electrodes for PSA detection, *J. Solid State Electrochem.* 25 (2021) 973–982.

- <https://doi.org/10.1007/s10008-020-04872-z>.
- [68] G. Ibáñez-Redín, N. Joshi, G.F. do Nascimento, D. Wilson, M.E. Melendez, A.L. Carvalho, R.M. Reis, D. Gonçalves, O.N. Oliveira, Determination of p53 biomarker using an electrochemical immunoassay based on layer-by-layer films with NiFe₂O₄ nanoparticles, *Microchim. Acta.* 187 (2020) 619. <https://doi.org/10.1007/s00604-020-04594-z>.
- [69] G. Ibáñez-Redín, E.M. Materon, R.H.M. Furuta, D. Wilson, G.F. do Nascimento, M.E. Melendez, A.L. Carvalho, R.M. Reis, O.N. Oliveira, D. Gonçalves, Screen-printed electrodes modified with carbon black and polyelectrolyte films for determination of cancer marker carbohydrate antigen 19-9, *Microchim. Acta.* 187 (2020) 417. <https://doi.org/10.1007/s00604-020-04404-6>.
- [70] A.S. Maghsoudi, S. Hassani, M.R. Akmal, M.R. Ganjali, K. Mirnia, P. Norouzi, M. Abdollahi, An electrochemical aptasensor platform based on flower-like gold microstructure-modified screen-printed carbon electrode for detection of serpin A12 as a Type 2 DIABETES BIOMARKER, *Int. J. Nanomedicine.* 15 (2020) 2219.
- [71] E. Povedano, V. Ruiz-Valdepeñas Montiel, M. Gamella, V. Serafín, M. Pedrero, L. Moranova, M. Bartosik, J.J. Montoya, P. Yáñez-Sedeño, S. Campuzano, J.M. Pingarrón, A novel zinc finger protein-based amperometric biosensor for miRNA determination, *Anal. Bioanal. Chem.* 412 (2020) 5031–5041. <https://doi.org/10.1007/s00216-019-02219-w>.
- [72] J. Sethi, M. Van Bulck, A. Suhail, M. Safarzadeh, A. Perez-Castillo, G. Pan, A label-free biosensor based on graphene and reduced graphene oxide dual-layer for electrochemical determination of beta-amyloid biomarkers, *Microchim. Acta.* 187 (2020) 288. <https://doi.org/10.1007/s00604-020-04267-x>.
- [73] V. Singh, Quantum dot decorated multi-walled carbon nanotube modified electrochemical sensor array for single drop insulin detection, *Mater. Lett.* 254 (2019) 415–418. <https://doi.org/https://doi.org/10.1016/j.matlet.2019.07.122>.
- [74] P. Karami, H. Bagheri, M. Johari-Ahar, H. Khoshsafar, F. Arduini, A. Afkhami, Dual-modality impedimetric immunosensor for early detection of prostate-specific antigen and myoglobin markers based on antibody-molecularly imprinted polymer, *Talanta.* 202 (2019) 111–122. <https://doi.org/https://doi.org/10.1016/j.talanta.2019.04.061>.
- [75] Y. Si, J.W. Park, S. Jung, G.-S. Hwang, Y.E. Park, J.E. Lee, H.J. Lee, Voltammetric layer-by-layer biosensor featuring purine nucleoside phosphorylase and chitosan for inosine in human serum solutions, *Sensors Actuators B Chem.* 298 (2019) 126840. <https://doi.org/https://doi.org/10.1016/j.snb.2019.126840>.
- [76] G. Ibáñez-Redín, R.H.M. Furuta, D. Wilson, F.M. Shimizu, E.M. Materon, L.M.R.B. Arantes, M.E. Melendez, A.L. Carvalho, R.M. Reis, M.N. Chaur, D. Gonçalves, O.N. Oliveira Jr, Screen-printed interdigitated electrodes modified with nanostructured carbon nano-onion films for detecting the cancer biomarker CA19-9, *Mater. Sci. Eng. C.* 99 (2019) 1502–1508. <https://doi.org/https://doi.org/10.1016/j.msec.2019.02.065>.
- [77] Y. Wang, J. Luo, J. Liu, S. Sun, Y. Xiong, Y. Ma, S. Yan, Y. Yang, H. Yin, X. Cai, Label-free microfluidic paper-based electrochemical aptasensor for ultrasensitive and simultaneous multiplexed detection of cancer biomarkers, *Biosens. Bioelectron.* 136 (2019) 84–90. <https://doi.org/https://doi.org/10.1016/j.bios.2019.04.032>.
- [78] S. Guerrero, D. Cadano, L. Agüí, R. Barderas, S. Campuzano, P. Yáñez-Sedeño, J.M. Pingarrón, Click chemistry-assisted antibodies immobilization for

- immunosensing of CXCL7 chemokine in serum, *J. Electroanal. Chem.* 837 (2019) 246–253. <https://doi.org/https://doi.org/10.1016/j.jelechem.2019.02.043>.
- [79] A. Valverde, A. ben Hassine, V. Serafín, C. Muñoz-San Martín, M. Pedrero, M. Garranzo-Asensio, M. Gamella, N. Raouafi, R. Barderas, P. Yáñez-Sedeño, S. Campuzano, J.M. Pingarrón, Dual Amperometric Immunosensor for Improving Cancer Metastasis Detection by the Simultaneous Determination of Extracellular and Soluble Circulating Fraction of Emerging Metastatic Biomarkers, *Electroanalysis*. 32 (2020) 706–714. <https://doi.org/https://doi.org/10.1002/elan.201900506>.
- [80] T. Putnin, A. Ngamaroonchote, N. Wiriyakun, K. Ounnunkad, R. Laocharoensuk, Dually functional polyethylenimine-coated gold nanoparticles: a versatile material for electrode modification and highly sensitive simultaneous determination of four tumor markers, *Microchim. Acta.* 186 (2019) 305. <https://doi.org/10.1007/s00604-019-3370-4>.
- [81] S. Chen, Z. Wang, X. Cui, L. Jiang, Y. Zhi, X. Ding, Z. Nie, P. Zhou, D. Cui, Microfluidic Device Directly Fabricated on Screen-Printed Electrodes for Ultrasensitive Electrochemical Sensing of PSA, *Nanoscale Res. Lett.* 14 (2019) 71. <https://doi.org/10.1186/s11671-019-2857-6>.
- [82] C. Varodi, F. Pogacean, M. Coros, M.-C. Rosu, R.-I. Stefan-van Staden, E. Gal, L.-B. Tudoran, S. Pruneanu, S. Mirel, Detection of 8-Hydroxy-2'-Deoxyguanosine Biomarker with a Screen-Printed Electrode Modified with Graphene, *Sensors* . 19 (2019). <https://doi.org/10.3390/s19194297>.